Quarkonia in High Energy Nuclear Collisions

Yunpeng Liu
Department of Physics, Tianjin University,
Tianjin 300072, P. R. China

Kai Zhou
Institute for Theoretical Physics,
Johann Wolfgang Goethe-University Frankfurt,
Max-von-Laue-Str.1, 60438 Frankfurt am Main, Germany
zhou@th.physik.uni-frankfun.de

Pengfei Zhuang
Physics Department,
Tsinghua University and Collaborative
Innovation Center of Quantum Matter,
Beijing 100084, P. R. China
Zhuangpf@fsinghua.edu.cn

We first review the cold and hot nuclear matter effects on quarkonium production in high energy collisions, then discuss three kinds of models to describe the quarkonium suppression and regeneration: the sequential dissociation, the statistical production and the transport approach, and finally make comparisons between the models and the experimental data from heavy ion collisions at SPS, RHIC and LHC energies.

1. Introduction

Phase transition is a key question in the study of many body systems in both theory and experiment. For nuclear matter, one of the most important topics is the confinement-deconfinement phase transition where hadrons melt into quarks and gluons at high temperature and/or high baryon density (evidence of the phase transition was found even before the quark model[1]). Although such a phase transition is widely accepted, there are still some open and fundamental questions. On the theoretical side, the confinement is not proved rigorously from the quantum chromodynamics (QCD) itself yet, and most discussions are based on computer simulations or effective models. On the experimental side, free quarks are not observed, and the

only experiment we can do on the earth is the relativistic heavy ion collisions, where two heavy nuclei collide with each other at extremely high energy to produce the hot and dense quark–gluon plasma (QGP). However, this new state of matter can not be measured directly, and one needs sensitive probes to show its existence in the early stage of heavy ion collisions.

J/ψ is one of the suggested probes to the QGP in relativistic heavy ion collisions. Unlike light quarks which are largely produced through soft processes in medium, heavy quarks are mainly created through hard processes in the initial stage and can interact with the quark matter strongly and has a chance to survive the hot and/or dense medium. As a result of the color screening effect, J/ψ suppression was suggested by Matsui and Satz in 1986[2] and observed at SPS in 1996,[3] which was regarded as an evidence of the QGP formation.

As a baseline of the quarkonium production in nuclear collisions, the first question to answer is how a quarkonium is produced in nucleon–nucleon collisions. A quarkonium is composed of a pair of heavy quarks, and the production of heavy quarks requires large Q^2, which can be calculated by perturbative QCD. At high energies, the dominant source for the heavy quark production at partonic level is the gluon fusion. Several programs are available like FONLL,[4,5] PYTHIA[6–8] and HIJING.[9,10] While the heavy quark production can well be studied in the pQCD framework, the subsequent formation of a quarkonium bound state as a color singlet hadron is a more complicated nonperturbative process, which is not yet understood clearly from first principle QCD theory. It is worth noting that this soft color neutralization process is much slower compared with the heavy quark hard production, due to the typical time scale hierarchy $\tau_{\text{quarkonium}} \sim 1/\epsilon_{\text{binding}} \gg \tau_{Q\bar{Q}} \sim 1/(2m_Q)$. Therefore, the quantum interference between the two stages are suppressed, which enables us to factorize the heavy quarkonium formation into the heavy quark production and the nonperturbative transition probability. Different phenomenological models and effective field theories are developed to describe this transition, like the color-singlet model (CSM),[11] the color-evaporation model (CEM),[12–15] and the nonrelativistic QCD (NRQCD).[16,17] We refer the readers to Refs. 11, 14, 17–19 for more details.

The quarkonium production in nuclear collisions is strongly affected by the nuclear matter. Before the hard processes for the heavy quark production, the parton distribution in a nucleus is different from the distribution in a nucleon due to the shadowing effect,[20] and the multi scattering of the partons with the surrounding nucleons, called Cronin effect,[21] modifies again the parton momentum distribution. After the $Q\bar{Q}$ pairs are created, they suffer from nuclear absorption[22,23] via the collisions with the spectators. All these nuclear effects happen before the hot medium formation and are called as cold nuclear matter effects. They are widely discussed in many theoretical models[19,24–28] and can be experimentally measured in p–A and d–A collisions[29–32] where a hot medium is not expected at low energies. The produced quarkonia will further be influenced by the hot nuclear matter effects when they pass through the created fireball. On one hand, they are suppressed by

inelastic interactions with partons in quark matter and hadrons in hadron matter. On the other hand, quarkonia with low momentum can also be regenerated in the fireball, and the regeneration becomes even dominant when the colliding energy is high enough. To study the properties of quarkonia at finite temperature and density, people take normally lattice QCD and effective field theories. In the spectrum functions from lattice calculation, the peak of J/ψ vanishes at around $1.5T_c$,[33–39] where T_c is the critical temperature of the deconfinement phase transition. For the effective models, we refer the readers to Refs. 40–42.

In this article, we focus on the phenomenological models on nuclear matter effects on quarkonium production and the comparison with the experimental data in high energy nuclear collisions at SPS, RHIC and LHC energies. We first discuss different cold and hot nuclear matter effects, then introduce three kinds of phenomenological models to describe the quarkonium evolution in A+A collisions: the sequential screening, the statistical model, and the transport approach, and finally make comparison between the models and the experimental data. We summarize and give a short outlook in the end.

2. Cold and Hot Nuclear Matter Effects

Although the main goal of the relativistic heavy ion collision is to study the properties of the QGP, it is necessary to discuss the cold nuclear matter effect first, which can hardly be separated in experiments from the hot nuclear matter effects. For quarkonium, there are mainly three cold nuclear matter effects as follows.

2.1. *Nuclear absorption*

The suppression of J/ψ due to hot nuclear matter effects was predicted in theory first.[2,43] Later on the suppression was observed at SPS energy in collisions of small nuclei.[44–47] However, it is found that the suppression can well be explained by the absorption of the nucleons.[48] For uniform nuclei, the length of the path in the two nuclei that the J/ψ passes through after its production is

$$L = \frac{3}{4}(R_1 + R_2), \tag{1}$$

where R_1 and R_2 are the radii of the nuclei. The normal suppression of J/ψ versus the length L is shown in Fig. 1. It can be seen that all the data lies in the same line, and the suppression can be interpreted as the dissociation of the J/ψ by the nucleons successively, so that the survival probability

$$S = e^{-\rho\sigma_{\rm abs}L}, \tag{2}$$

where ρ is the nuclear density, and $\sigma_{\rm abs}$ is the nuclear absorption cross section. The value of $\sigma_{\rm abs}$ is several mb at SPS energy.[43] Such a effect is usually measured in $p+{\rm A}$ collisions to determine the $\sigma_{\rm abs}$ and applied to ${\rm A}+{\rm A}$ collisions.

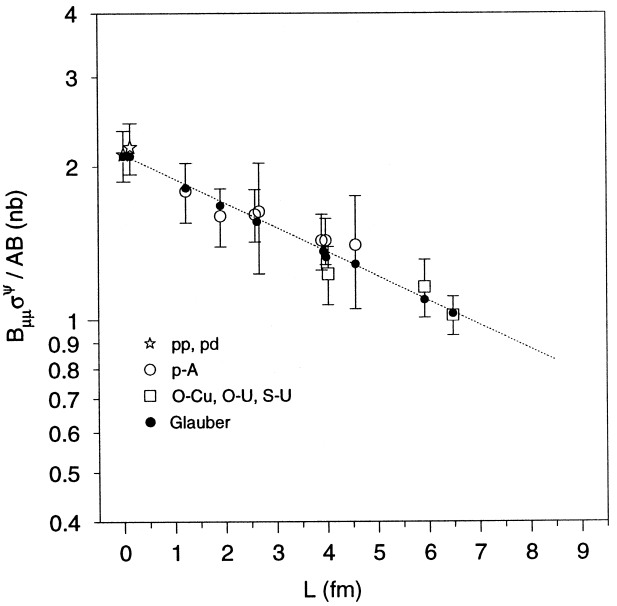

Fig. 1. The normal suppression of J/ψ at SPS energy as a function of the length L. σ^{ψ}, $B_{\mu\mu}$ are the cross section and the branch ratio of J/ψ to dimuon, respectively, and A and B are the mass numbers of the two nuclei. Figure from Ref. 22.

The time for the two nuclei to pass through each other can roughly be estimated as $t_{\rm pass} \sim 2Rm_N/\sqrt{s_{\rm NN}}$, where m_N and $\sqrt{s_{\rm NN}}$ are the mass of a nucleon and the center of mass energy of one nucleon pair. At RHIC energy it is about 0.06 fm/c, which is far smaller than the formation time of J/ψ. At LHC energy, this time is even smaller by one order of magnitude. Therefore, considering a non-zero quarkonium formation time $\tau_{\rm form} \sim 1/\epsilon_{\rm binding}$, the $\sigma_{\rm abs}$ is not simply the cross section between a fully developed J/ψ and a nucleon in vacuum. Instead it reflects the interaction between the nucleons and some preliminary state of J/ψ before it is formed. The nuclear absorption effect is less and less important with increasing collision energy as shown in Fig. 2 for the fitted $\sigma_{\rm abs}(\sqrt{s_{\rm NN}})$.[24] It is recently found that the normal suppression of ψ' is much stronger than that of J/ψ at RHIC energy,[49] and a quantitative explanation is still lacking.

2.2. *Nuclear shadowing*

As mentioned in the introduction, the heavy quark production is a perturbative process and is dominated by the gluon fusion at high energy. Thus the yield of the heavy quarkonia is closely related to the parton distribution function of gluons in the initial colliding nuclei. Considering the subprocess

$$g_1 + g_2 \to J/\psi + X, \tag{3}$$

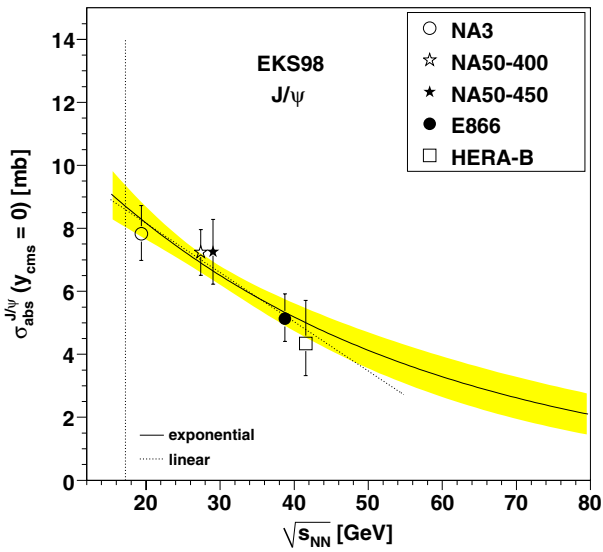

Fig. 2. The collision energy dependence of J/Ψ nuclear absorption cross section $\sigma_{\rm abs}^{J/\psi}$. Figure from Ref. 24.

where g_1 and g_2 are two gluons in the nucleons, then the on shell condition of particle X reads

$$m_X^2 = x_1 x_2 s_{\rm NN} - (x_1 + x_2)\sqrt{s_{\rm NN}} m_T \cosh y + (x_1 - x_2)\sqrt{s_{\rm NN}} m_T \sinh y + m_\psi^2 \tag{4}$$

where it is assumed that both g_1, and g_2 are massless so that the longitudinal momentum and the energy of the subprocess are $(x_1 - x_2)\sqrt{s_{\rm NN}}/2$ and $(x_1 + x_2)\sqrt{s_{\rm NN}}/2$, respectively, with x_1, x_2, $\sqrt{s_{\rm NN}}$ being the momentum fraction of g_1 and g_2 and the center of mass energy of the nucleons, and m_ψ, m_T, y are the mass, transverse mass and rapidity of the J/ψ, respectively. If the particle X (usually being gluon) is also massless ($m_X = 0$), then the above equation gives the relation between x_1 and x_2 as[50]

$$x_2 = \frac{x_1 m_T \sqrt{s_{\rm NN}} e^{-y} - m_\psi^2}{\sqrt{s_{\rm NN}}(x_1\sqrt{s_{\rm NN}} - m_T e^{y})}. \tag{5}$$

Furthermore, if the four-momentum of X can be omitted, corresponding to the leading order of the Color Evaporation Model (CEM), both x_1 and x_2 can be determined by the momentum information of the final J/ψ,

$$x_{1,2} = \frac{m_T}{\sqrt{s_{\rm NN}}} e^{\pm y}. \tag{6}$$

Therefore, the transverse momentum and rapidity distribution of J/ψ is determined by not only the cross section of the gluon fusion subprocess, but also the parton distribution functions for gluon in the initial particles. The distribution

function f_i^A of parton i in a nucleus differs from a simple superposition of the distribution function f_i in a free nucleon. Such nuclear shadowing is usually described by the modification factor $R_i^A(x,\mu_F) = f_i^A(x,\mu_F)/(Af_i(x,\mu_F))$, where μ_F is the factorization scale for the hard process. Higher energy collisions concern smaller x physics, which usually locate at stronger shadowing region. Therefore, parton shadowing effect plays an important role in high energy collisions.

There are different parameterizations of the change of parton distribution functions: EKS98,[51] EPS08,[52] EPS09,[53] nDS,[54] and so forth. Such a shadowing effect can be measured in p+A collisions, especially in the rapidity dependence of the nuclear modification factor. For more details we refer the readers to Refs. 28, 50–55.

2.3. *Cronin effect*

The momentum distribution of quarkonia in p+A collisions is different from that in $p+p$ collisions. That is the Cronin effect, which was named after Cronin and firstly observed for light hadrons.[21] Due to the Cronin effect, part of the low momentum quarkonia are shifted to the intermediate momentum, so that the yield of the low momentum quarkonia is suppressed, and that of the intermediate ones are enhanced in nuclear collisions.

The Cronin effect of J/ψ can be interpreted as a gluon kicking by the surrounded nucleons in transverse direction before the fusion of the two gluons into a J/ψ. The transverse momentum broadening is proportional to the length l that the gluons pass through in the nuclei, and the transverse momentum distribution in A+A collisions reads

$$f_{AA}(\mathbf{p}_T) = \int d\mathbf{k} f_k(\mathbf{k}) f_{pp}(\mathbf{p}_T - \mathbf{k}), \tag{7}$$

where $\mathbf{k}$ is the transverse momentum increase of the gluons due to the scattering, which follows a Gaussian distribution since it is due to multi-scattering. Taking average over the transverse momentum square on both sides of above equation, one find that

$$\langle p_T^2\rangle_{AA} = \langle p_T^2\rangle_{pp} + \langle k^2\rangle, \tag{8}$$

where the average are for the distributions of f_{AA}, f_{pp} and f_k, respectively, and it is assumed that at least one of f_{pp} and f_k is isotropic, which is usually true. The momentum increase can be taken as Gaussian since it is accumulated from multi-scattering, and it is proportional to l,

$$\langle k^2\rangle = a_{gN} l, \tag{9}$$

where the parameter a_{gN} is about $0.1\,\mathrm{GeV}^2/\mathrm{fm}$ at RHIC.[56] If the transverse momentum of J/ψ is not too large so that f_{pp} can be described by a Gaussian distribution, f_{AA} is simply

$$f_{AA}(\mathbf{p}_T) = \frac{\langle p_T^2\rangle_{pp}}{\langle p_T^2\rangle_{AA}} f_{pp}\left(\sqrt{\frac{\langle p_T^2\rangle_{pp}}{\langle p_T^2\rangle_{AA}}}\mathbf{p}_T\right). \tag{10}$$

2.4. *Color screening*

The screening effect is well known in the electric plasma, and it also happens in the QGP. One significant difference is that the temperature T to form QGP is far larger than the masses of its components, while the electric plasma is typically non-relativistic. As a result, the temperature dependence of the screening effect differs qualitatively. It is well known that the screening mass μ of a Coulomb potential can be expressed as

$$\mu = \sqrt{\frac{4\pi\alpha \sum_i Q_i^2 \rho_i}{T}}, \tag{11}$$

where α, Q_i, ρ_i and T are the fine structure constant, the charge number of particle i, the density of particle i, and the temperature of the plasma, respectively. In the non-relativistic case, the density of charged particles is fixed, and the only factor to compete with the screening is the kinetic energy of the charged particles. Therefore the higher the temperature is, the weaker the screening is, and $\mu \propto T^{-1/2}$. In the contrary, the density of the partons increases with temperature in QGP. If the mass of the partons is omitted $\rho_i \propto T^3$, and the screening mass is $\mu \propto T$, so that the higher the temperature is, the stronger the screening effect is. When the temperature is strong enough, the heavy quark pair breaks up and the quarkonium is dissociated. More details will be discussed in Subsec. 3.1.

2.5. *Gluon dissociation*

The photon disintegration of QED bound state like hydrogen atoms is well studied. Similarly, a quarkonium can be dissociated by a gluon. The cross section was calculated first by Peskin with operator production expansion.[57] The result is introduced in Subsec. 3.3. There are three main differences between the hydrogen and the quarkonium dissociation: (1) the coupling constant is small for QED and large for QCD, which makes it difficult to calculate the cross section in high accuracy; (2) the final state interaction is comparable with the attraction in the bound state for the QED, while it is one order of magnitude smaller in quarkonium, because the heavy quarks are in color singlet state in the quarkonium and in color octet state after the quarkonium is dissociated; (3) the three gluon interaction has equal contribution as the quark–gluon interaction at leading order, which is absent in QED. Many efforts were made to understand the quarkonium suppression better after Peskin. The cross section for excited states were calculated later.[58,59] The recoil effect was considered in Ref. 59. The same cross section was reproduced by a pQCD calculation[60] with a quarkonium to heavy quark pair vertex which is from Bathe–Saltpeter equation. By this method, the high-order contribution was also calculated.[61] The correction due to final state interaction was also discussed.[62] The cross section beyond the dipole approximation was calculated in Ref. 63.

2.6. *Quasi-free scattering*

The gluon dissociation $g + (Q\bar{Q}) \to Q + \bar{Q}$ is the leading order process, which is important at low temperature when the binding energy is large. When the temperature is high, the quasi-free scattering is believed to be important[56,64] since the quarks are loosely bounded. In high temperature limit, the heavy quarks can no longer form a quarkonium as in the color screening scenario, which was also implied by the lattice result. A T matrix method was developed to calculate the suppression based on heavy quark potential and the scattering theory, which can adopt the lattice potential directly.[65]

3. Phenomenology

In order to link the properties of quarkonia and the experimental results, plenty of phenomenological research has been done. In the following we will introduce three popular models for quarkonia production and/or suppression in the hot medium.

3.1. *Sequential dissociation model*

One of the earliest models for heavy quarkonium suppression is the sequential dissociation model,[2,66] which assumes that the quarkonia are dissociated sequentially when the temperature of the quark matter increases, since those quarkonia with small binding energy are more fragile. Taking advantage of the heavy mass of the constituent quarks, the interaction between the heavy quarks can be described by a potential. In vacuum, the Cornell potential works well

$$V(r) = -\frac{\alpha}{r} + \sigma r, \tag{12}$$

which contains a Coulomb part at small radius r and a linear part at large r. The former is the result of one gluon exchange potential which comes from the leading order perturbation, and the latter gives the confinement which is non-perturbative. The Schrödinger equation of charm quarks reads

$$\left[-\frac{\nabla^2}{2\mu} + V(r)\right]\psi = E\psi, \tag{13}$$

where μ is the reduced mass of the two heavy quarks. Solving the above equation, it was found in Ref. 67 that the mass spectra of quarkonia can well be reproduced with parameters $m_c = 1.25\,\text{GeV}$, $m_b = 4.65\,\text{GeV}$, and $\alpha = \pi/12$ and $\sigma = 0.2\,\text{GeV}^2$ in the Cornell potential. See Table 1.

At finite temperature, the free energy approximately takes the form[68]

$$F(r) = -\frac{\alpha}{r}e^{-\mu r} - \frac{\sigma}{2^{3/4}\Gamma(3/4)}\left(\frac{r}{\mu}\right)^{1/2} K_{1/4}(\mu^2 r^2) - \mu + \frac{\sigma}{2^{3/2}\mu}\frac{\Gamma(1/4)}{\Gamma(3/4)}, \tag{14}$$

Table 1. Mass M and binding energy ϵ of heavy quarkonia in vacuum calculated from Cornell potential. Table from Ref. 67.

States	J/ψ	χ_c	ψ'	$\Upsilon(1S)$	$\Upsilon(1P)$	$\Upsilon(2S)$	$\Upsilon(2P)$	$\Upsilon(3S)$
M/GeV	3.10	3.53	3.68	9.46	9.99	10.02	10.26	10.36
ϵ/GeV	0.64	0.20	0.05	1.10	0.67	0.54	0.31	0.20
error/GeV	0.02	−0.03	0.03	0.06	−0.06	−0.06	−0.08	−0.07

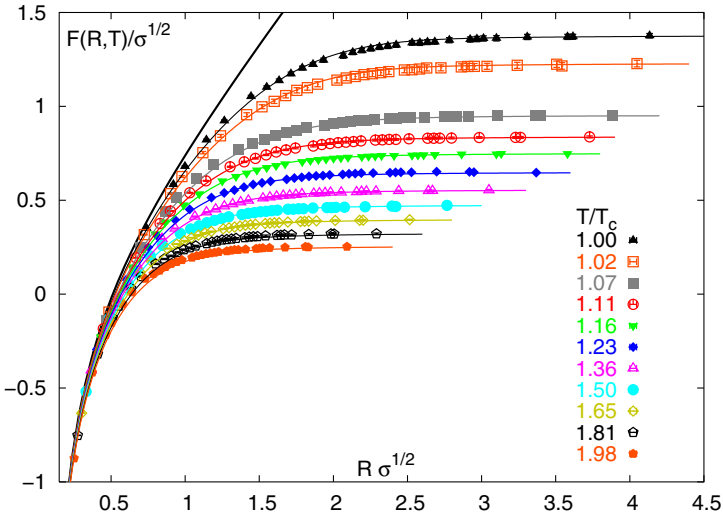

Fig. 3. (Color online) The fit potential of the free energy from Lattice QCD. Figure from Ref. 67.

where all the temperature dependence lies in $\mu = \mu(T)$. It is found that this formula can fit the free energy obtained from the LQCD simulation well,[67] as shown in Fig. 3. We further find that $\mu(T)$ above T_c can be parameterized as

$$\frac{\mu(\bar{T})}{\sqrt{\sigma}} = k\bar{T} + a\sigma_t\sqrt{\frac{\pi}{2}}\left[\mathrm{erf}\left(\frac{b}{\sqrt{2}\sigma_t}\right) - \mathrm{erf}\left(\frac{b-\bar{T}}{\sqrt{2}\sigma_t}\right)\right],$$

where $\bar{T} \equiv T/T_c$, and the dimensionless parameters are $k = 0.587$, $a = 2.150$, $b = 1.054$ and $\sigma_t = 0.07379$.

One can also derive the internal energy

$$U = F - T\frac{\partial F}{\partial T} \tag{15}$$

from the above free energy. The potential is in principle between the free energy limit and the internal energy limit. In the free energy limit, the heavy quark pair can exchange heat with the medium immediately, and in the internal limit the they can not. Taking the potential V in Eq. (13) either as the free energy F or as the potential U will give an extreme limit for the properties of quarkonia. The dissociation temperatures of heavy quarkonia and those of B_c mesons are listed as in Tables 2 and 3, respectively. It can be seen that The dissociation temperature T_d

Table 2. The ratio of the dissociation temperature T_d to the critical temperature T_c of different charmonium and bottomonium states in the internal energy limit $V = U$ and the free energy limit $V = F$. Part of data are from Ref. 67.

States	J/ψ	χ_c	ψ'	$\Upsilon(1S)$	$\Upsilon(1P)$	$\Upsilon(2S)$	$\Upsilon(2P)$	$\Upsilon(3S)$
$V = U$	2.26	1.16	1.11	7.0	3.15	2.98	2.05	1.98
$V = F$	1.16	≤ 1	≤ 1	2.90	1.12	≤ 1	≤ 1	≤ 1

Table 3. The ratio of the dissociation temperature T_d to the critical temperature T_c of different B_c states in the internal energy limit $V = U$ and the free energy limit $V = F$. Part of data are from Ref. 69.

States		$B_c(1S)$	$B_c(1P)$	$B_c(2S)$	$B_c(1D)$
M/GeV		6.36	6.72	6.90	6.98
T_d/T_c	$V = U$	3.27	1.59	1.41	1.17
	$V = F$	1.51	≤ 1	≤ 1	≤ 1

differs significantly between $V = U$ and $V = F$. In the $V = U$ limit, the T_d of J/ψ is above the temperature at SPS, and near to the highest temperature at RHIC. In the $V = F$ limit, it is little above the critical temperature and most of the J/ψs are supposed to dissociate at RHIC energy. As to Υ, no suppression of the 1S state is expected even in the $V = F$ limit. The results for B_c mesons lies between J/ψ and Υ.

Lattice QCD simulation also gives some results on the dissociation temperature of quarkonia from the spectrum function. For J/ψ it is around $1.5T_c$, above which the peak of J/ψ in the spectrum function disappears.[33]

One should keep in mind that the above results are based on the assumption of static heavy quarks. Since the quarkonia produced in high energy nuclear collisions have a typical transverse momentum of several GeV, one should consider the charmonium velocity dependence of the color screening. From the lattice calculation of the charmonium spectral function, the J/ψ suppression is stronger at high p_T,[70] while some phenomenological study including the relaxation time of medium for the color screening indicates an increasing dissociation temperature with J/ψ velocity relative to the medium, which means a less quarkonium suppression at high p_T.[71] The experimental results can be better described by the latter. The velocity dependence of the ratio T_d/T_c predicted by Ref. 71 is shown in Fig. 4.

In the above, the medium is assumed as isotropic, and it can not be true at the early stage of the heavy ion collision. It is found that the screening effect is weaker in an anisotropic medium,[72] which make it easier for the quarkonia to survive the QGP. Recently, the relativistic modification is also discussed in the potential model by solving the Schrödinger equation.[73]

The sequential dissociation model was supported by the experiments for Υ suppression at RHIC[74,75] and the double ratio at LHC.[76]

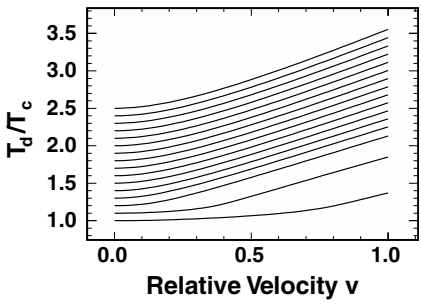

Fig. 4. The velocity dependence of the ratio of dissociation temperature to critical temperature T_d/T_c of heavy quarkonia in QGP.

3.2. *Statistical model*

Soon after the sequential dissociation model, a totally different model was suggested that the yield of J/ψ is determined by the statistics.[77–81] The statistical model was used to describe the light hadrons and made a great success.[82] Then it was applied to charmonia with the consideration of charm quark conservation, which gives the basic equation of the statistical model for heavy flavors[77]

$$N_{Q\bar{Q}} = \frac{1}{2}N_{\rm o} + N_{\rm h}, \tag{16}$$

where $N_{Q\bar{Q}}$, $N_{\rm o}$ and $N_{\rm h}$ are the number of initially produced heavy quark pairs, final open heavy flavors and final hidden heavy flavors, respectively. This equation not only require net charmness conservation, but also require conservation of charm and anticharm quarks separately. $N_{\rm o}$ and $N_{\rm h}$ are determined by the statistics.

In the grand canonical ensemble, the numbers on the right-hand side are

$$N_{\rm o}^{\rm gr} = g\rho_{\rm o}V, \tag{17}$$

$$N_{\rm h}^{\rm gr} = g^2\rho_{\rm h}V, \tag{18}$$

where g is the fugacity, and $\rho = \sum_i \rho_i^{th}$ is the total density as a summation of the thermal density over all the open or hidden particles under consideration.

Since the fireball in heavy ion collisions is isolated, a canonical ensemble describes better the system. The difference is negligible when the number of heavy quarks $N_{Q\bar{Q}}$ is large, but it becomes important when $N_{Q\bar{Q}}$ is comparable with or even smaller than unit. In the canonical ensemble the numbers of the heavy flavor is expressed as[81]

$$N_{\rm o}^{\rm ca} = g\rho_{\rm o}V\frac{I_1(g\rho_{\rm o}V)}{I_0(g\rho_{\rm o}V)}, \tag{19}$$

$$N_{\rm h}^{\rm ca} = g^2\rho_{\rm h}V, \tag{20}$$

where I_1 and I_0 are modified Bessel functions of the first kind. $I_1(x)/I_0(x)$ approaches to 1 when x approaches to positive infinity, and it approaches to $x/2$ when x approaches to zero. Therefore when the number of charm quarks is large, it

approaches the grand canonical ensemble limit. On the other hand, if the number of charm quarks is small then a much larger fugacity g is required to balance the two sides of Eq. (16), which leads to an enhancement of the quarkonium production. Such a canonical enhancement was studied for strangeness before,[83] and it can also be obtained by solving the main equation for number of charm quark distribution, and taking the long time limit to reach the thermal equilibrium, which proved Eq. (19) elegantly with the help of the generating function.[84]

Now let us calculate the yield of hidden heavy flavors explicitly under some approximations. We note that the yield of quarkonia is far smaller than that of the open heavy hadrons, therefore, to determine the fugacity we can safely neglect the N_h term in Eq. (16). As a result we obtain $g = 2N_{Q\bar{Q}}/(\rho_0 V)$ and

$$N_h = \frac{4\rho_h N_{Q\bar{Q}}^2}{\rho_0^2 V} \tag{21}$$

in the large $N_{Q\bar{Q}}$ limit. If $N_{Q\bar{Q}}$ is small instead, we obtain $g^2 = 4N_{Q\bar{Q}}/(\rho_0^2 V^2)$ and

$$N_h = \frac{4\rho_h N_{Q\bar{Q}}}{\rho_0^2 V}. \tag{22}$$

To include both limits, the yield reads

$$N_h = \frac{4\rho_h N_{Q\bar{Q}}^2}{\rho_0^2 V}\left(1 + \frac{1}{N_{Q\bar{Q}}}\right). \tag{23}$$

On the one hand, the basic assumption of the statistical model for heavy flavor is the heavy quark pair conservation, as indicated by Eq. (16). On the other hand, the statistics counts the contribution of arbitrary number of heavy quark pairs. A consequent question comes up: how different number of quark pairs contribute to a single collision. The event by event fluctuation answers this question as suggested by Ref. 85. Considering one event, the yield of heavy quarkonia N_h is proportional to the collision rate between Q and $\bar{Q}$, and thus for a given volume

$$N_h \propto N_Q N_{\bar{Q}} = N_{Q\bar{Q}}^2, \tag{24}$$

where $N_{Q\bar{Q}}$ is a random variable which fluctuates from event to event. When we average events we have $\langle N_h \rangle \propto \langle N_{Q\bar{Q}}^2 \rangle$. Since $N_{Q\bar{Q}}$ comes from plenty of independent nucleon–nucleon collisions, it follows Poisson distribution, and for Poisson distribution we have

$$\langle N_{Q\bar{Q}}^2 \rangle = \langle N_{Q\bar{Q}} \rangle^2 \left(1 + \frac{1}{\langle N_{Q\bar{Q}} \rangle}\right). \tag{25}$$

It means that the correction at small $N_{Q\bar{Q}}$ due to event by event fluctuation is the factor $1 + 1/\langle N_{Q\bar{Q}} \rangle$,[69] which is consistent with Eq. (23) where the average brackets are not written explicitly.

Another question one has to answer is why Eq. (23) is not extensive with the fluctuation considered. Actually the correction term $1/N_{Q\bar{Q}}$ comes from the correlation of the existence of Q and $\bar{Q}$, that is whenever there is a heavy quark, there

is also a heavy antiquark in the volume which increases the yield of heavy quarkonia. However, if the quark and antiquark are too far away, then they will not see each other and it no longer helps to produce the quarkonia. Therefore only when they lie in some correlation volume,[83,86] this effect can contribute. Such a correlation volume was taken as the volume of the fireball within unit rapidity bin in most statistical models[80] and was more carefully considered in a transport model.[86] Recently, a detailed study further considered both the correlation in the coordinate space and that in the momentum space to determine the correlation (or effective) volume.[87] It is found that in the classical limit, the correlation volume increases linearly with time at the short time limit, and then it increases with time more slowly, and in the long time limit the correlation volume increases with $t^{3/2}$. Here the "short" time and the "long" time are compared with the average time between collisions of the heavy quark with the particles in the medium. It also implies that the formation time and size of the initial wave package of the heavy quarks can be important in this problem.

The coalescence model made great success for light hadrons[88–92] and were also used to describe the production of heavy quarkonia, whose results is similar to that of the statistical model. The basic idea is to project the quark states to the hadron states with the help of their Wigner functions. For heavy quarkonium production in the coalescence model, one may refer to Refs. 93 and 94. In a recent study, the triply charmed baryon Ω_{ccc} is even predicted in the heavy ion collisions at LHC.[95]

3.3. *Transport model*

Different from the sequential dissociation model and the statistical model, the transport model[64,69,86,96–99] contains the information of time evolution of the quarkonia. As an approximation, the quarkonia can be described by the distribution function $f(\mathbf{x}, \mathbf{p}, t)$ in phase space, which respects the classical Boltzmann equation

$$\delta_t f + \mathbf{v} \cdot \nabla f - (\nabla U) \cdot \nabla_p f = -\alpha f + \beta + C, \tag{26}$$

where $\mathbf{v}$, U, α, β, C are the velocity of the quarkonium, the potential that the quarkonia feels in the medium, the dissociation rate of the quarkonium, the regeneration rate of the quarkonium and the elastic collision term, respectively. Almost all the transport models are solving some simplified version of such a transport equation.

The effect of mean field U was discussed in Ref. 100, and the elastic collision is regarded as small in most of discussions, which is implied by the small v_2 of J/ψ at RHIC.[101] Without the potential term and the elastic collisions term, the above equation can be written in a explicitly boost invariant form as

$$\cosh(y-\eta)\delta_\tau f + \mathbf{v}_T \cdot \nabla_T f + \frac{1}{\tau}\sinh(y-\eta)\delta_\eta f = -\alpha_T f + \beta_T, \tag{27}$$

where $y = (1/2)\ln[(E+p_z)/(E-p_z)]$, $\eta = (1/2)\ln[(t+z)/(t-z)]$, $\mathbf{v}_T = \mathbf{p}_T/E_T$ and $\tau = \sqrt{t^2 - z^2}$ are the momentum rapidity, spacetime rapidity, transverse

velocity and the longitudinal proper time of the quarkonium, respectively, and $E_T = \sqrt{M^2 + \mathbf{p}_T^2}$ is the transverse energy. $\mathbf{v}_T = \mathbf{p}_T/E_T$, $\alpha_T = \alpha E/E_T$, and $\beta_T = \beta E/E_T$ are all boost invariant as long as the medium is boost invariant. The solution of the above equation is

$$\begin{aligned} f(&\mathbf{p}_T, y, \mathbf{x}_T, \eta, \tau) \\ &= f(\mathbf{p}_T, y, \mathbf{X}_T(\tau_0), H(\tau_0), \tau_0) e^{-\int_{\tau_0}^{\tau} d\tau' \alpha(\mathbf{p}_T, y, \mathbf{X}_T(\tau'), H(\tau'), \tau')/\Delta(\tau')} \\ &\quad + \int_{\tau_0}^{\tau} d\tau' \beta(\mathbf{p}_T, y, \mathbf{X}_T(\tau'), H(\tau'), \tau')/\Delta(\tau') \\ &\quad \times e^{-\int_{\tau'}^{\tau} d\tau'' \alpha(\mathbf{p}_T, y, \mathbf{X}_T(\tau''), H(\tau''), \tau'')/\Delta(\tau'')} \end{aligned} \tag{28}$$

with

$$\begin{aligned} \mathbf{X}_T(\tau') &= \mathbf{x}_T - \mathbf{v}_T[\tau \cosh(y - \eta) - \tau' \Delta(\tau')], \\ H(\tau') &= y - \operatorname{arcsinh}[(\tau/\tau') \sinh(y - \eta)], \\ \Delta(\tau') &= \sqrt{1 + (\tau/\tau')^2 \sinh^2(y - \eta)}, \end{aligned} \tag{29}$$

and $\mathbf{x}_T = (x, y)$. Here we have only changed the variables and the physical meaning of f is the same as that in Eq. (26). The two terms of the solution are for the initially produced quarkonia and the regenerated quarkonia, respectively. Both of them suffer anomalous suppression that is represented by the exponential terms.

Taking the approximation $\eta \approx y$, the transport equation can be further simplified to be

$$\delta_\tau f + \mathbf{v}_T \cdot \nabla_T f = -\alpha_T f + \beta_T, \tag{30}$$

and the simplified solution is

$$\begin{aligned} f(&\mathbf{p}_T, y, \mathbf{x}_T, \eta, \tau) \\ &= f(\mathbf{p}_T, y, \mathbf{X}_T(\tau_0), \eta, \tau_0) e^{-\int_{\tau_0}^{\tau} d\tau' \alpha(\mathbf{p}_T, y, \mathbf{X}_T(\tau'), \eta, \tau')} \\ &\quad + \int_{\tau_0}^{\tau} d\tau' \beta(\mathbf{p}_T, y, \mathbf{X}_T(\tau'), \eta, \tau') e^{-\int_{\tau'}^{\tau} d\tau'' \alpha(\mathbf{p}_T, y, \mathbf{X}_T(\tau''), \eta, \tau'')} \end{aligned} \tag{31}$$

with

$$\mathbf{X}_T(\tau') = \mathbf{x}_T - \mathbf{v}_T(\tau - \tau'). \tag{32}$$

If a local equilibrium is reached, the left-hand side of Eq. (30) vanishes, and the corresponding distribution function f_0 satisfies

$$0 = -\alpha_T f_0 + \beta_T. \tag{33}$$

Thus the transport equation (30) can be rewritten as

$$\delta_\tau f + \mathbf{v}_T \cdot \nabla_T f = -\alpha_T (f - f_0). \tag{34}$$

If all the other particles that destroy or produce quarkonia are in thermal equilibrium, then f_0 is the thermal distribution, otherwise f_0 can in general deviate from

the thermal distribution. If the coordinate dependence of α_T and β_T is neglected, integrating Eq. (30) over the coordinate space, one obtains

$$\delta_\tau f_p = -\alpha_{Tp} f_p + \beta_{Tp}, \tag{35}$$

which describes the time evolution of the momentum spectrum f_p of quarkonia. If the momentum dependence of α and β is further neglected, namely consider a momentum averaged dissociation and regeneration rates Γ and G, the rate equation is generally written as

$$\frac{dN_\Psi}{d\tau} = -\Gamma N_\psi + G. \tag{36}$$

The second term on the left-hand side of Eq. (30) is kinetic, which leads to the leakage effect[102] so that high p_T quarkonia are more likely to escape the fireball and suffer less suppression. As a result, the transverse momentum increases after the transport.

The two terms on the right-hand side contains the interaction between the quarkonium and the medium. If the temperature is relatively low and quarkonia are tightly bound states, the gluon dissociation process $g + (Q\bar{Q}) \rightarrow Q + \bar{Q}$ is important. Peskin calculated the cross section for the $1S$ state by operator product expansion,[57] and it reads

$$\sigma_{1S} = A_0 \frac{(\omega/\epsilon_{1\mathrm{S}} - 1)^{3/2}}{(\omega/\epsilon_{1\mathrm{S}})^5} \tag{37}$$

with

$$A_0 = \frac{2^{11}\pi}{3N_c^2\sqrt{m_Q^3\epsilon_{1S}}}, \tag{38}$$

where ω, ϵ_{1S}, N_c and m_Q are the energy of gluon in the quarkonia rest frame, the binding energy of the quarkonia, the number of color and the mass of a heavy quark, respectively. For such a process the dissociation rate is

$$\alpha_T = \int \frac{d\mathbf{k}}{(2\pi)^3 E_T} \sigma_{1S} F_{g(Q\bar{Q})} f_g(k), \tag{39}$$

where $F_{g(Q\bar{Q})} = \sqrt{(p\cdot k)^2 - m_{(Q\bar{Q})}^2 m_g^2}$ and f_g are the flux factor and the distribution function of gluons, respectively, with k being the momentum of gluons. The cross section of Υ is shown in Fig. 5 as an example, where the cross section for the excited states are from Refs. 58 and 59. It can be seen that the binding energy for the $\Upsilon(1S)$ state is large while that for the excited states are smaller. Meanwhile, the amplitude of the cross section is also much larger for the excited states. Therefore the excited states are more likely to be dissociated in a medium with the temperature to be several hundred MeV. This is qualitatively consistent with the color screening scenario.

However, the gluon dissociation process is not the same as the color screening. To see this more clearly one can consider the classical electric analog, where the

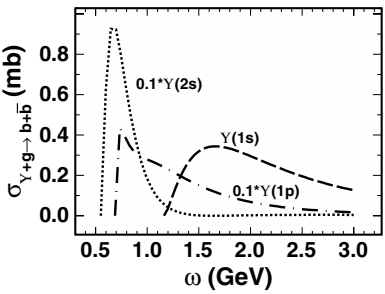

Fig. 5. The cross section for $g + \Upsilon \to b + \bar{b}$.[57–59]

number of charged particles are fixed. In the low temperature limit, the charged particle are closely around the test charge, and the screening is strong. However, in this case the photons are rare and their energies are small which can hardly break a bound state. In the high temperature limit, the screening radius becomes large due to the stronger thermal motion of the particles in the medium, while both the number of photons increases and the average energy of each photon increases, which make it easier to break a bound state. The only reason that the gluon dissociation behaves similar to that of the color screening is that the number of charged particles in heavy ion collisions increases with temperature since the temperature is comparable with the mass of the blocks of the medium. Therefore, it is necessary

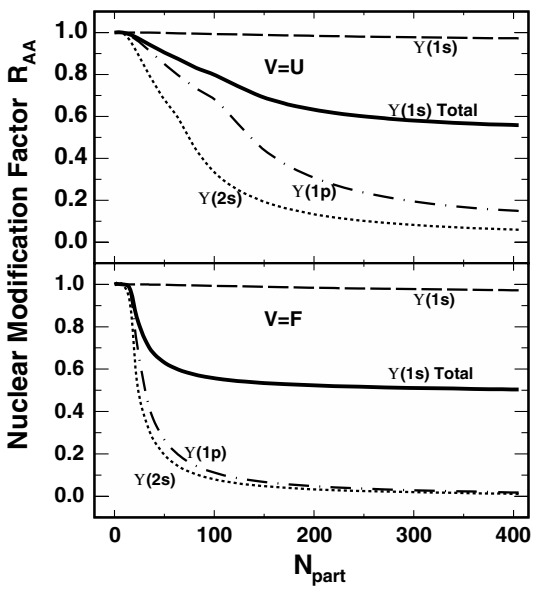

Fig. 6. The nuclear modification factor of $\Upsilon(1S)$ as a function of the number of participant $N_{\rm part}$ predicted by a transport model at RHIC energy. The upper and lower panels are from $V = U$ and $V = F$, respectively. Figure from Ref. 103.

to include the color screening effect besides the scattering process. In some models, this is done by introducing the dissociation temperature T_d of the quarkonia above which a quarkonium dissociates in the medium immediately, and the dissociation temperature can be determined from the potential model as in Subsec. 3.1. The nuclear modification factor for Υ at RHIC is shown in Fig. 6.

The regeneration rate β_T is related to the dissociation rate with the detail balance principle,[98] and thus it depends on the distribution of charm quarks. The motion of charm quarks was widely studied.[104–108] The simplest case is that the momentum distribution of the heavy quarks is thermal. However this may not be true, especially for bottom. An ansatz was suggested that the non-thermal distribution in momentum space will suppress the regeneration process that is related to the relaxation time,[56,109] which was verified by a cascade model[110] later. Recently the modification of initially produced quarkonia due to the change of the distribution function of the heavy quarks from interaction with the medium was

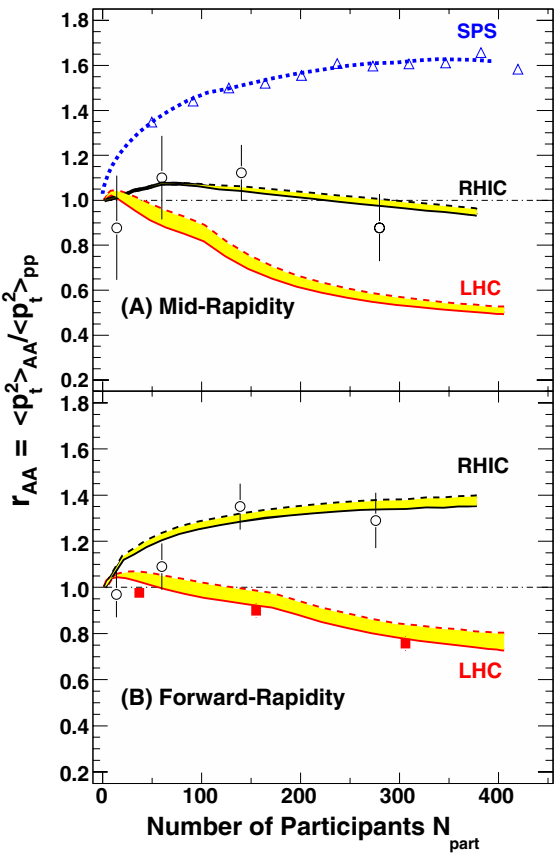

Fig. 7. (Color online) The ratio of $\langle p_T^2 \rangle$ in A–A collisions to that in pp collisions as a function of centrality at different colliders. This figure is from Ref. 116. Data from Refs. 117–120.

discussed in Ref. 111. The influence of the formation time[112] and the event-by-event fluctuation[113] were discussed by the same authors. As in the statistical model, the canonical enhancement should also be considered in the regeneration. The results from a cascade simulation of the heavy quarks[87] shows that the correlation of the heavy quarks in the phase space from the primary hard collisions can also be important, especially when the heavy quarks are rare. Thermal production of the charm quarks were also discussed[114,115] which depends on the initial temperature of the fireball much.

One advantage of the transport model is to study the momentum of quarkonia. It is found that although the nuclear modification factor R_{AA} is similar among SPS energy, RHIC energy and LHC energy at forward rapidity, the ratio

$$r_{AA} \equiv \frac{\langle p_T^2 \rangle_{AA}}{\langle p_T^2 \rangle_{pp}} \tag{40}$$

is sensitive to the origin of J/ψs and thus differs much among SPS, RHIC and LHC.[116] At SPS energy, the initially produced J/ψs are dominant, and therefore the r_{AA} increases with the number of participant $N_{\rm part}$ due to the hot nuclear matter effects and the leakage effect.[102] At RHIC energy, the regenerated J/ψs will play a role in the most central collisions with relatively small transverse momentum due to the thermalization of charm quarks.[98] As a result, the transverse momentum increases with $N_{\rm part}$ first and then decreases with $N_{\rm part}$ when $N_{\rm part}$ is large.[121] At LHC energy, the regenerated J/ψs are much more important, and the contribution is larger and larger for more central collisions, which leads to the continuous decrease of r_{AA}. For the same reason, the r_{AA} is larger at forward rapidity due to less regeneration. This effect was discussed in Ref. 116 and shown in Fig. 7.

4. Comparison with the Experimental Results

In this part we review some results of above models on heavy quarkonium production and suppression compared with the experiments in relativistic heavy ion collisions. Although the J/ψ is mostly discussed, there are a family of quarkonia that we are interested in. Both masses and quantum numbers of them are shown in Table 4. It can be seen that the mass of them are above 3 GeV for charmonia and above 9 GeV for bottomonia, which are high above the temperature of the fireball produced in heavy ion collisions. Only the quarkonia under threshold are listed and the quarkonia of η_c and η_b are not included in this table because they have large width even in vacuum. For example, the width of η_c in vacuum is about 32 MeV that is more than three hundred times larger compared with the width 93 keV of J/ψ. The small widths of J/ψ and $\Upsilon(1S)$ are guaranteed by the J^{PC}, and they can only decay through three gluons in QCD and thus suppressed by the OZI rule,[124] and the excited states can decay directly and/or indirectly to the ground state. Since the binding energy of J/ψ and $\Upsilon(1S)$ is far above the critical temperature T_c for the deconfinement phase transition, they are expected to survive the

Table 4. Mass M, binding energy ϵ, Spin J, parity P, and charge conjugate C of the quarkonium families. The data come from Particle Data Group.[122]

Constituent quarks	Quarkonia	M/GeV	ϵ/GeV	J^{PC}
$(c\bar{c})$	$J/\psi(1S)$	3.097	0.642	1^{--}
	$\chi_{c0}(1P)$	3.415	0.324	0^{++}
	$\chi_{c1}(1P)$	3.511	0.228	1^{++}
	$\chi_{c2}(1P)$	3.556	0.183	2^{++}
	$\psi(2S)$	3.686	0.053	0^{--}
$(b\bar{b})$	$\Upsilon(1S)$	9.460	1.099	1^{--}
	$\chi_{b0}(1P)$	9.859	0.700	0^{++}
	$\chi_{b1}(1P)$	9.893	0.666	1^{++}
	$\chi_{b2}(1P)$	9.912	0.647	2^{++}
	$\Upsilon(2S)$	10.023	0.536	1^{--}
	$\Upsilon(1D)$	10.164	0.395	2^{--}
	$\chi_{b0}(2P)$	10.232	0.327	0^{++}
	$\chi_{b1}(2P)$	10.255	0.304	1^{++}
	$\chi_{b2}(2P)$	10.269	0.290	2^{++}
	$\chi_{b2}(3S)$	10.355	0.204	2^{++}
	$\chi_b(3P)$	10.534	0.025	$?^{?+}$
$(c\bar{b})^\dagger$	B_c^+	6.276	0.873	1^{--}

Note: †Although B_c meson is not a quarkonium as it contains quarks of different flavors, we also list it here because it is similar to heavy quarkonia in the sense that both quarks are heavy in B_c. For discussions on B_c meson, one may refer to Refs. 69, 85 and 123.

QGP as a probe, accompanied with the suppression especially for the excited states whose binding energies are relatively small and thus they are more fragile in the hot medium.

4.1. *Observables*

A quarkonium is a neutral particle, and it can not be observed directly. The decay channel of dileptons are mostly used to measure the quarkonia. The fraction for different channels are shown in Table 5. By measuring the momenta of the lepton pairs, it is possible to reconstruct the quarkonia according to the invariant mass and measure their momenta. Meanwhile the spin of a quarkonium can also be

Table 5. Decay channels and the branch ratios of J/ψ and $\Upsilon(1S)$.

Decay channel	Branch ratio
$J/\psi \to e^+ + e^-$	5.97%
$J/\psi \to \mu^+ + \mu^-$	5.96%
$\Upsilon \to e^+ + e^-$	2.38%
$\Upsilon \to \mu^+ + \mu^-$	2.48%

measured, and this has been done in N–N collisions.[125–127] Although the spin of the quarkonium may help in heavy ion collisions,[128] there is no public data available at present yet. Therefore the current data are all based on either the total yield or the momentum distribution of quarkonia.

Following the original idea by Satz, the most measured observable is the nuclear modification factor

$$R_{AA} \equiv \frac{N_{AB}}{T_{AB}\sigma_{pp}} \tag{41}$$

as a function of centrality, which is usually characterized by the number of participant $N_{\rm part}$ or the number of binary collisions $N_{\rm coll}$. In the above, N_{AB} is the yield of heavy quarkonia in A–A collisions and T_{AB} is the overlap function of the two colliding nuclei, and σ_{pp} is the quarkonium production cross section in pp collisions. This observable is less than unit in nucleus–nucleus collisions from SPS energy to LHC energy up to now.

To look into the details, the momentum dependence is also measured. In the longitudinal direction, the momentum is usually converted to rapidity

$$y \equiv \frac{1}{2}\ln\frac{E+p_z}{E-p_z}, \tag{42}$$

since on one hand it is additive under successive boost along z direction,[a] and on the other hand it is closely related to pseudo-rapidity which is simply a function of the angle between the outgoing particles and the beam and thus related to the position of detectors. For example, the detectors at Phenix only measure the J/ψs at mid rapidity ($|y| < 0.9$), and those at forward rapidity ($1.2 < y < 2.2$).[129] In the transverse direction $R_{AA}(\mathbf{p}_T)$ can be measured, where $\mathbf{p}_T \equiv (p_x, p_y)$ is the transverse momentum of a quarkonium. At RHIC energy the transverse momentum can be measured up to about 10 GeV.[130]

The angular distribution along the transverse direction is described as the elliptic flow

$$v_2 = \left\langle \frac{p_x^2 - p_y^2}{p_x^2 + p_y^2} \right\rangle = \langle \cos 2\phi \rangle, \tag{43}$$

which is the second Fourier coefficients. For light hadrons the elliptic flow has well been measured,[131–134] and discussed a lot, which comes from the non-isotropic properties of the medium and is not expected in N–N collisions.

Besides, we are also interested in the beam energy dependence, which put quarkonia into the fireball with different initial temperatures and densities. In the following we will review some important results from three typical beam energy scale, $\sqrt{s} = 17.3$ A GeV at SPS, $\sqrt{s} = 200$ A GeV at RHIC and $\sqrt{s} = 2.76$ A GeV at LHC, respectively.

[a]In the point of view of group theory, a boost can be expressed as e^{yK}, where K is the boost generator of the Lorentz group, and the rapidity y is the boost parameter, and thus it is additive.

4.2. *SPS*

At SPS energy, J/ψ suppression was observed in experiments[22,46,47] after the theoretical prediction.[2] As shown in Fig. 1, the normal suppression can well be explained by the absorption of J/ψ by the nucleons at SPS. A similar suppression was also observed in d+A or p+A collisions at RHIC and LHC,[49,135] although the formation time of J/ψ is larger than the time for a J/ψ to pass through the primary nuclear matter. The (effective) cross section $\sigma_{\rm abs}$ is about several mb.[56,86,136,137] It is not well understand why the normal suppression for ψ' is much stronger than that of J/ψ,[49] but some model predicts that the high energy density could lead to even stronger suppression of ψ' in the most central p+Pb collisions at LHC energy due to the hot nuclear matter effects if there is any.[138]

The anomalous suppression was also observed.[3,139] A transport model calculation[109] is shown in Fig. 8 compared with the experimental data.[139] The obvious deviation from the normal suppression implies that J/ψ suffers some other suppression other than the cold nuclear matter effect. It was widely recognized as a smoking gun of the formation of QGP. Note that the anomalous suppression was observed only in central Pb+Pb collisions, but not in smaller system or the peripheral collisions. It can be estimated that the temperature of the fireball is not far above the critical temperature T_c of deconfinement phase transition. It is natural to expect stronger suppression at RHIC and LHC if the only hot nuclear matter effect is color screening. However this is not the fact as it was found later.

Accompanied with the suppression of J/ψ its transverse momentum spectrum also changes.[30] The average transverse momentum square $\langle p_T^2 \rangle$ was found to be larger in central Pb+Pb collisions.[30] Similar effect is also observed in p+A collisions and also for light hadrons at intermediate p_T, known as Cronin effect.[21] The hot nuclear matter effect will also affect the transverse momentum spectrum, since high

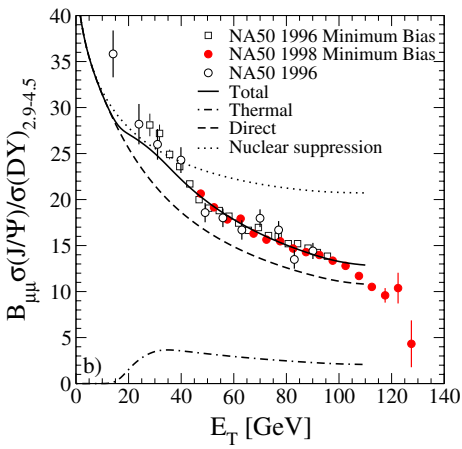

Fig. 8. (Color online) The anomalous suppression of J/ψ. The data is from NA50,[139] and both the calculation and the figure are from Ref. 109.

p_T J/ψ may left the fireball earlier and suffer less suppression, which is called the leakage effect.[102] The behavior of the transverse momentum dependence of the nuclear modification factor is consistent with the above two mechanisms that R_{AA} is larger at high p_T and smaller at low p_T.

ψ' is also measured,[30,140] which makes it possible to compare with the statistical model directly. It can be seen from Fig. 9[141] that the anomalous suppression of ψ' is stronger than that of J/ψ, and the statistical model describes well the ratio of them. It is necessary to keep in mind that excited states are more fragile than the ground state, and when we consider the suppression of inclusive J/ψs as measured in most cases, the suppression of the excited states has significant contribution besides the ground state itself. About 30% of the inclusive J/ψs are from the decay from χ_c, and 10% from ψ'[142,b] whose binding energies are smaller as shown in Table 4. The transverse momentum of ψ' is higher than that of J/ψ at top SPS energy,[30] which implies that a low p_T ψ' is more likely to be destroyed by the hot medium.

4.3. *RHIC*

The centrality dependence of the nuclear modification factor R_{AA} of J/ψ at middle rapidity is shown in Fig. 10. The high transverse momentum calculations ($p_T >$ 5 GeV) are predictions. In the full p_T calculations, the suppression of J/ψ is strong even in the peripheral collisions, and both transport models can describe the data well. For the high p_T results, both transport models predicted a smaller suppression, which also agrees with the data qualitatively. This implies that high p_T J/ψs suffers

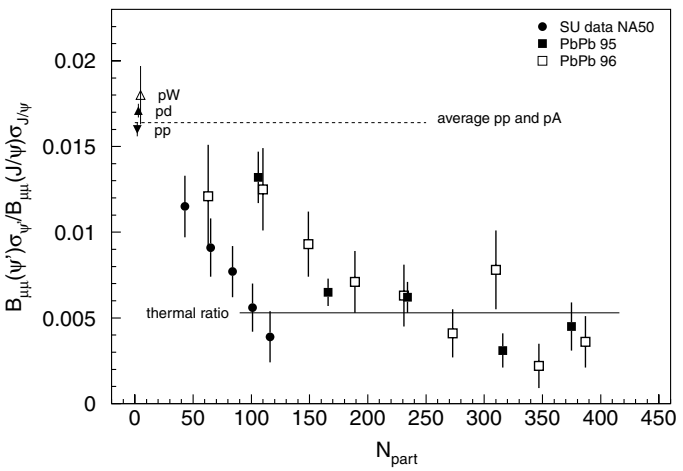

Fig. 9. The anomalous suppression of J/ψ and ψ' at SPS. The "expected" in the figure is the yield with normal suppression included. The data are from NA50,[22,136] and both the calculation and the figure are from Ref. 77.

[b]This ratio is also true for higher energies as implied by the CEM model and the experiments, see Refs. 143 and 144 for example.

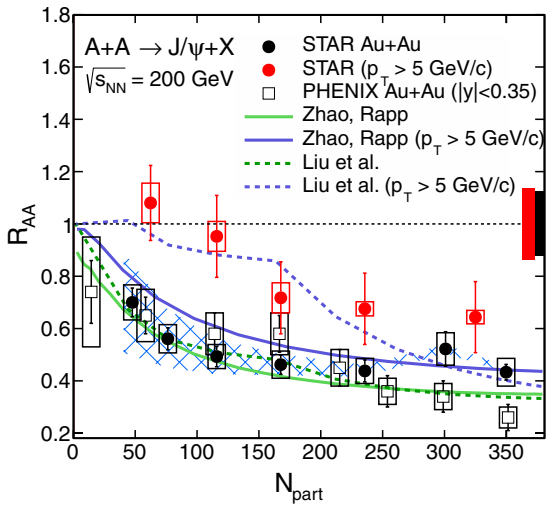

Fig. 10. (Color online) Nuclear modification factor R_{AA} of J/ψ as a function of the number of participant $N_{\rm part}$ at middle rapidity at RHIC. The calculations are from transport models.[121,145] Data from Refs. 130 and 146, and figure from Ref. 147.

less suppression. The centrality dependence of J/ψ suppression in Cu + Cu collisions was also measured, and the $N_{\rm part}$ dependence of R_{AA} is similar to that in Au + Au collisions.[148]

At RHIC energy, quarkonia are measured at both middle rapidity and forward rapidity. Fig. 11 shows the rapidity dependence of R_{AA} both at middle rapidity and at forward rapidity. Different from a naive screening scenario, the suppression at forward rapidity is stronger than that at middle rapidity in both centrality bins.

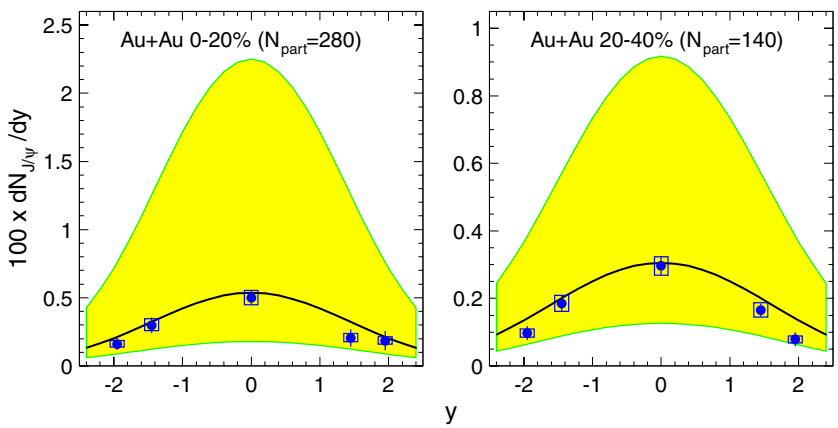

Fig. 11. (Color online) The rapidity dependence of R_{AA} at RHIC from the statistical model[79] compared with experimental data[119] at centralities 0–20% (left) and 20–40% (right). The bands show the uncertainty due to the input cross section of the model. Figure from Ref. 79.

In heavy ion collisions, more energy is deposited at middle rapidity. Therefore the temperature at forward rapidity is not expected to be higher than that at middle rapidity. The results here implies the regeneration of J/ψ as we have discussed in the previous section, since there are more charm quarks at middle rapidity, which leads to larger contribution to the thermal production. When the same idea is applied in the transport model, the rapidity dependence can also be explained qualitatively.[99]

In order to learn more information on the dynamics of J/ψ suppression and regeneration, the transverse momentum dependence of R_{AA} were calculated and measured. It is shown in Fig. 12. Compared with the experimental data are the results from two transport models.[121,145] Both models can explain the data at present. It can be seen that the suppression of J/ψ is stronger at low p_T than that at high p_T as at SPS energy. The PHENIX data also show a valley structure in most centrality bins. This non-monotonic structure can be an evidence of the regeneration,[121] but it needs to be further confirmed since the current data are still with relatively large uncertainty. At $p_T = 3\,\text{GeV}$, there is a large difference between the data from PHENIX and that from STAR in the most central and most peripheral collisions. The nuclear modification factor of J/ψs with high p_T was well measured by STAR,[130] and it confirms that a J/ψ with high p_T suffers less suppression, which is consistent of the leading order gluon dissociation cross section[57,149] and the idea of relaxation of the color screening.[71]

The elliptic flow v_2 is a measure of the collective motion. The v_2 of J/ψ was also measured recently by STAR as shown by Fig. 13. It can be seen from this

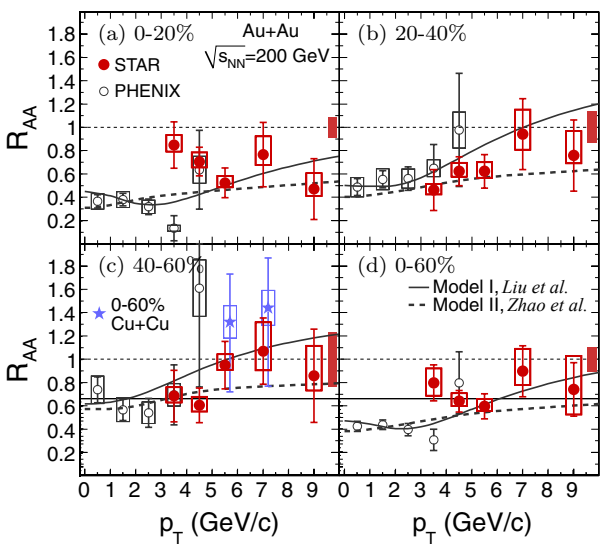

Fig. 12. (Color online) The nuclear modification factor R_{AA} of J/ψ as a function of the transverse momentum p_T at RHIC energy. The data[130] are measured by STAR and PHENIX. The two curves are due to Refs. 121 and 145. Figure from Ref. 147.

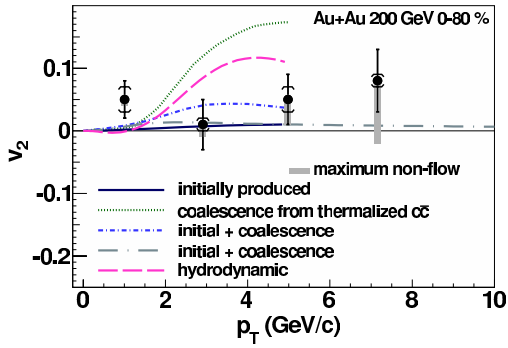

Fig. 13. (Color online) The elliptic flow v_2 of J/ψ as a function of the transverse momentum p_T at RHIC. Figure from STAR in Ref. 101.

figure that the v_2 of J/ψ is far smaller than that of light hadrons like pion, and it is also smaller than what the coalescence model or hydrodynamics predicted, which implies that the J/ψ is far from thermalization at RHIC energy, and the initially produced J/ψ plays an important role in observables. The curves are from models correspond to Refs. 98, 94, 150–152, respectively. We note here that the elliptic flow is measured at peripheral collisions. Although the regeneration is small in this centrality, it can still play an important role in central collisions at RHIC.

Υ was also measured by STAR,[74,75,153] and it is found that the suppression of Υ is consistent with the simple assumption that all the excited Υ states melts up and all the ground state survives as suggested by the sequential dissociation model.

4.4. *LHC*

In peripheral collisions the suppression at LHC is similar to that at middle rapidity at RHIC, while in the most central collisions the R_{AA} is larger than that at RHIC, which is different from the color screening scenario. Similar to RHIC energy, the R_{AA} at middle rapidity at LHC is also larger than that at forward rapidity.[154] The R_{AA} in the most central collisions is about 0.8[154] at middle rapidity, while the R_{AA} for high p_T J/ψs is around 0.2 in the most central collisions.[155] All the observations above implies the important contribution of the regeneration of J/ψ at LHC energy.

The transverse momentum dependence of J/ψ also shows that the R_{AA} is large at low p_T and relatively small at high p_T,[154] which is totally different from that at SPS and RHIC energy. The elliptic flow v_2 of J/ψ at LHC energy[156] is shown in Fig. 14. It can be seen that there is a peek around $p_T = 3\,\text{GeV}$, which was never observed at RHIC energy. Since the elliptic flow is a measure of the collective motion, such a non-zero v_2 implies either the J/ψ get thermalized in the fireball or the regenerated charmonia contribute a lot to the final detected J/ψs. The rapidity dependence of R_{AA} also shows that it decreases with rapidity even at the forward

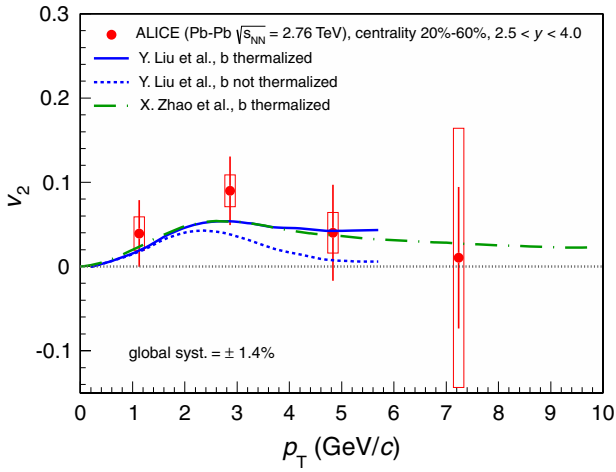

Fig. 14. (Color online) The elliptic flow v_2 of J/ψ at LHC energy as a function of the transverse momentum p_T compared with calculation from transport models.[151,160] Figure from Ref. 156.

bins.[154] All these momentum measures are consistent with the regeneration of J/ψ at LHC.

The excited states were also well measured. The double ratio of Υ shows a significant stronger suppression for excited Υs relative to $\Upsilon(1S)$,[76] which is an analog of the charmonia at SPS. The double ratio of charmonia is measured by ALICE[157] and CMS.[158] According to the CMS data, the double ratio at high p_T increases with $N_{\rm part}$ monotonically, and it is even far larger than unit for 3GeV $< p_T <$ 30GeV and $1.6 < y < 2.4$. Most of the data can be explained by the transport model with B meson decay[159] except those above unit.

5. Outlook

In this paper, we review the progress of heavy quarkonia in relativistic heavy ion collisions. The study of heavy quarkonia has made great progress during the last several decades, and the topic is becoming broader and broader. The study of J/ψ has been extended to its excited states, the Υ families and even B_c mesons. The production of heavy quarks is related to the perturbative QCD, and the formation of quarkonia is related to the hadronization. The suppression and regeneration of quarkonia are related to the interaction inside the hot quark matter, and the motion of heavy quarks and the suppression of heavy quarkonia are similar to jet quenching. The observable of quarkonia is actually dileptons and the production of regenerated quarkonia is also similar to that of the dileptons.

Many observables have been measured, such as the nuclear modification factor $R_{AA}(p_T)$, $R_{AA}(N_{\rm part})$, $R_{AA}(y)$, $R_{AA}(L)$, the double ratio, the transverse momentum square $\langle p_T^2 \rangle$, the elliptic flow $v_2(p_T)$. The beam energy ranges from 17.3 GeV

at SPS to 2.76 TeV at LHC. It can be expected that the energy scan at RHIC and the new experiment of FAIR will generate more results about heavy quarkonia.

On the theoretical side, most of the data can be explained qualitatively. Besides the color screening, many new concepts are developed in the theoretical calculations, like the statistical production of quarkonia, the canonical ensemble effect, the regeneration, the velocity dependence of the dissociation temperature, and the correlation between the heavy quarks.

There are still a lot of open questions to be answered in both experiment and theory. For experiments, the direct evidence of the regeneration, that is the enhancement of heavy quarkonia in A–A collisions, may be found for B_c meson[69,123] and Ω_{ccc}[95] at LHC energy. The spin degree of freedom of quarkonia is not measured in A–A collisions, which may contain more information about quarkonium formation. The precision for open heavy flavor and high p_T quarkonia is to be improved. For theorist, the mechanism of heavy quarkonia production is still to be determined. The strong suppression of excited charmonia in p–A and high multiplicity pp collisions at LHC is still to be understood. Of course, a more important question to answer is what properties of the medium we can learn from the heavy quarkonia.

Acknowledgments

The work is supported by the NSFC and MOST grant Nos. 11335005, 2013CB922000 and 2014CB845400.

References

1. R. Hagedorn, *Nuovo Cim. Suppl.* **3** (1965) 147–186.
2. T. Matsui and H. Satz, *Phys. Lett. B* **178** (1986) 416.
3. M. Gonin *et al.*, *Nucl. Phys. A* **610** (1996) 404c–417c.
4. M. Cacciari, M. Greco and P. Nason, *JHEP* **9805** (1998) 007.
5. M. Cacciari, S. Frixione and P. Nason, *JHEP* **0103** (2001) 006.
6. T. Sjostrand, *Comput. Phys. Commun.* **82** (1994) 74–90.
7. T. Sjostrand, S. Mrenna and P. Z. Skands, *JHEP* **0605** (2006) 026.
8. T. Sjostrand, S. Mrenna and P. Z. Skands, *Comput. Phys. Commun.* **178** (2008) 852–867.
9. X.-N. Wang and M. Gyulassy, *Phys. Rev. D* **44** (1991) 3501–3516.
10. X.-N. Wang and M. Gyulassy, *Phys. Rev. D* **45** (1992) 844–856.
11. C.-H. Chang, *Nucl. Phys. B* **172** (1980) 425–434.
12. H. Fritzsch, *Phys. Lett. B* **67** (1977) 217.
13. F. Halzen, *Phys. Lett. B* **69** (1977) 105.
14. J. Amundson, O. J. Eboli, E. Gregores and F. Halzen, *Phys. Lett. B* **372** (1996) 127–132.
15. J. Amundson, O. J. Eboli, E. Gregores and F. Halzen, *Phys. Lett. B* **390** (1997) 323–328.
16. W. Caswell and G. Lepage, *Phys. Lett. B* **167** (1986) 437.
17. G. T. Bodwin, E. Braaten and G. P. Lepage, *Phys. Rev. D* **51** (1995) 1125–1171.
18. J. C. Collins, D. E. Soper and G. F. Sterman, *Adv. Ser. Direct. High Energy Phys.* **5** (1988) 1–91.

19. J. Lansberg, *Int. J. Mod. Phys. A* **21** (2006) 3857–3916.
20. A. H. Mueller and J.-W. Qiu, *Nucl. Phys. B* **268** (1986) 427.
21. J. W. Cronin *et al.*, *Phys. Rev. D* **11** (1975) 3105.
22. M. C. Abreu *et al.*, *Phys. Lett. B* **466** (1999) 408–414.
23. C. Gerschel and J. Hufner, *Phys. Lett. B* **207** (1988) 253–256.
24. C. Lourenco, R. Vogt and H. K. Woehri, *JHEP* **0902** (2009) 014.
25. R. Vogt, *Phys. Rev. C* **81** (2010) 044903.
26. R. Vogt, S. J. Brodsky and P. Hoyer, *Nucl. Phys. B* **360** (1991) 67–96.
27. R. Vogt, *Phys. Rept.* **310** (1999) 197–260.
28. R. Vogt, *Phys. Rev. C* **71** (2005) 054902.
29. M. Leitch *et al.*, *Phys. Rev. Lett.* **84** (2000) 3256–3260.
30. M. Abreu *et al.*, *Phys. Lett. B* **499** (2001) 85–96.
31. A. Adare *et al.*, *Phys. Rev. C* **91** (2015) 014907.
32. R. Aaij *et al.*, *JHEP* **1402** (2014) 072.
33. M. Asakawa and T. Hatsuda, *Phys. Rev. Lett.* **92** (2004) 012001.
34. M. Asakawa, T. Hatsuda and Y. Nakahara, *Prog. Part. Nucl. Phys.* **46** (2001) 459–508.
35. T. Umeda, R. Katayama, O. Miyamura and H. Matsufuru, *Int. J. Mod. Phys. A* **16** (2001) 2215.
36. O. Kaczmarek, F. Karsch, P. Petreczky and F. Zantow, *Phys. Lett. B* **543** (2002) 41–47.
37. R. Morrin, A. O Cais, M. Oktay, M. Peardon, J. Skullerud *et al.*, *PoS* **LAT2005** (2006) 176.
38. O. Kaczmarek and F. Zantow, *Phys. Rev. D* **71** (2005) 114510.
39. H. Ding *et al.*, *Phys. Rev. D* **86** (2012) 014509.
40. A. Bazavov, P. Petreczky and A. Velytsky, Quarkonium at finite temperature, in *Quark–Gluon Plasma 4*, eds. R. C. Hwa and X.-N. Wang (World Scientific, 2010), pp. 61–110.
41. N. Brambilla, A. Pineda, J. Soto and A. Vairo, *Rev. Mod. Phys.* **77** (2005) 1423.
42. N. Brambilla, A. Pineda, J. Soto and A. Vairo, *Nucl. Phys. B* **566** (2000) 275.
43. C. Gerschel and J. Hufner, *Z. Phys. C* **56** (1992) 171–174.
44. C. Baglin *et al.*, *Phys. Lett. B* **220** (1989) 471–478.
45. C. Baglin *et al.*, *Phys. Lett. B* **270** (1991) 105–110.
46. M. Abreu *et al.*, *Z. Phys. C* **38** (1988) 117.
47. M. Abreu *et al.*, *Phys. Lett. B* **449** (1999) 128–136.
48. D. Kharzeev and H. Satz, *Phys. Lett. B* **356** (1995) 365–372.
49. A. Adare *et al.*, *Phys. Rev. Lett.* **111**(20) (2013) 202301.
50. E. Ferreiro, F. Fleuret, J. Lansberg and A. Rakotozafindrabe, *Phys. Rev. C* **81** (2010) 064911.
51. K. Eskola, V. Kolhinen and C. Salgado, *Eur. Phys. J. C* **9** (1999) 61–68.
52. K. J. Eskola, H. Paukkunen and C. A. Salgado, *JHEP* **0807** (2008) 102.
53. K. Eskola, H. Paukkunen and C. Salgado, *JHEP* **0904** (2009) 065.
54. D. de Florian and R. Sassot, *Phys. Rev. D* **69** (2004) 074028.
55. E. Ferreiro, F. Fleuret, J. Lansberg and A. Rakotozafindrabe, *Phys. Lett. B* **680** (2009) 50–55.
56. X. Zhao and R. Rapp, *Phys. Lett. B* **664** (2008) 253–257.
57. M. E. Peskin, *Nucl. Phys. B* **156** (1979) 365.
58. X.-N. Wang and F. Yuan, *Phys. Lett. B* **540** (2002) 62–67.
59. A. Polleri, T. Renk, R. Schneider and W. Weise, *Phys. Rev. C* **70** (2004) 044906.
60. Y.-S. Oh, S. Kim and S. H. Lee, *Phys. Rev. C* **65** (2002) 067901.

61. Y. Park, K.-I. Kim, T. Song, S. H. Lee and C.-Y. Wong, *Phys. Rev. C* **76** (2007) 044907.
62. F. Brezinski and G. Wolschin, *Phys. Lett. B* **707** (2012) 534–538.
63. Y. Liu, C. M. Ko and T. Song, *Phys. Rev. C* **88**(6) (2013) 064902.
64. L. Grandchamp and R. Rapp, *Phys. Lett. B* **523** (2001) 60–66.
65. M. Mannarelli and R. Rapp, *Phys. Rev. C* **72** (2005) 064905.
66. F. Karsch, M. Mehr and H. Satz, *Z. Phys. C* **37** (1988) 617.
67. H. Satz, *J. Phys. G* **32** (2006) R25.
68. V. V. Dixit, *Mod. Phys. Lett. A* **5** (1990) 227.
69. Y. Liu, C. Greiner and A. Kostyuk, *Phys. Rev. C* **87** (2013) 014910.
70. H.-T. Ding, *Nucl. Phys. A* **904–905** (2013) 619c–622c.
71. Y. Liu, N. Xu and P. Zhuang, *Phys. Lett. B* **724** (2013) 73–76.
72. A. Dumitru, Y. Guo, A. Mocsy and M. Strickland, *Phys. Rev. D* **79** (2009) 054019.
73. X. Guo, S. Shi and P. Zhuang, *Phys. Lett. B* **718** (2012) 143–146.
74. R. Reed, *J. Phys. Conf. Ser.* **270** (2011) 012026.
75. L. Adamczyk *et al.*, *Phys. Lett. B* **735** (2014) 127.
76. S. Chatrchyan *et al.*, *Phys. Rev. Lett.* **107** (2011) 052302.
77. P. Braun-Munzinger and J. Stachel, *Phys. Lett. B* **490** (2000) 196–202.
78. A. Andronic, P. Braun-Munzinger and J. Stachel, *Phys. Lett. B* **673** (2009) 142–145.
79. A. Andronic, P. Braun-Munzinger, K. Redlich and J. Stachel, *Nucl. Phys. A* **789** (2007) 334–356.
80. A. Andronic, P. Braun-Munzinger, K. Redlich and J. Stachel, *Phys. Lett. B* **571** (2003) 36–44.
81. M. I. Gorenstein, A. Kostyuk, H. Stoecker and W. Greiner, *Phys. Lett. B* **509** (2001) 277–282.
82. A. Andronic, P. Braun-Munzinger and J. Stachel, *Acta Phys. Polon. B* **40** (2009) 1005–1012.
83. S. Hamieh, K. Redlich and A. Tounsi, *Phys. Lett. B* **486** (2000) 61–66.
84. C. Ko *et al.*, *Phys. Rev. Lett.* **86** (2001) 5438–5441.
85. A. Kostyuk, Double, triple and hidden charm production in the statistical coalescence model, arXiv:nucl-th/0502005.
86. L. Grandchamp, R. Rapp and G. E. Brown, *Phys. Rev. Lett.* **92** (2004) 212301.
87. Y. Liu, C. M. Ko and F. Li, Heavy quark correlations and the effective volume for quarkonia production, arXiv:1406.6648.
88. V. Greco, C. Ko and P. Levai, *Phys. Rev. Lett.* **90** (2003) 202302.
89. V. Greco, C. M. Ko and P. Levai, *Phys. Rev. C* **68** (2003) 034904.
90. R. C. Hwa and C. Yang, *Phys. Rev. C* **67** (2003) 034902.
91. R. Fries, B. Muller, C. Nonaka and S. Bass, *Phys. Rev. Lett.* **90** (2003) 202303.
92. D. Molnar and S. A. Voloshin, *Phys. Rev. Lett.* **91** (2003) 092301.
93. B. Zhang, *Phys. Lett. B* **647** (2007) 249–252.
94. V. Greco, C. M. Ko and R. Rapp, *Phys. Lett. B* **595** (2004) 202–208.
95. H. He, Y. Liu and P. Zhuang, *Phys. Lett. B* **746** (2015) 59–63.
96. R. L. Thews, M. Schroedter and J. Rafelski, *Phys. Rev. C* **63** (2001) 054905.
97. L. Grandchamp, S. Lumpkins, D. Sun, H. van Hees and R. Rapp, *Phys. Rev. C* **73** (2006) 064906.
98. L. Yan, P. Zhuang and N. Xu, *Phys. Rev. Lett.* **97** (2006) 232301.
99. Y. Liu, Z. Qu, N. Xu and P. Zhuang, *J. Phys. G* **37** (2010) 075110.
100. B. Chen, K. Zhou and P. Zhuang, *Phys. Rev. C* **86** (2012) 034906.
101. L. Adamczyk *et al.*, *Phys. Rev. Lett.* **111**(5) (2013) 052301.
102. P.-F. Zhuang and X. L. Zhu, *Phys. Rev. C* **67** (2003) 067901.

103. Y. Liu, B. Chen, N. Xu and P. Zhuang, *Phys. Lett. B* **697** (2011) 32–36.
104. K. Huggins and R. Rapp, *Nucl. Phys. A* **896** (2012) 24–45.
105. J. Uphoff, O. Fochler, Z. Xu and C. Greiner, *Phys. Rev. C* **84** (2011) 024908.
106. S. K. Das, F. Scardina, S. Plumari and V. Greco, *Phys. Rev. C* **90**(4) (2014) 044901.
107. S. Cao, G.-Y. Qin and S. A. Bass, *Phys. Rev. C* **88**(4) (2013) 044907.
108. X. Zhu, N. Xu and P. Zhuang, *Phys. Rev. Lett.* **100** (2008) 152301.
109. L. Grandchamp and R. Rapp, *Nucl. Phys. A* **709** (2002) 415–439.
110. T. Song, K. C. Han and C. M. Ko, *Phys. Rev. C* **85** (2012) 054905.
111. T. Song, *Phys. Rev. C* **89** (2014) 044903.
112. T. Song, C. M. Ko and S. H. Lee, *Phys. Rev. C* **87** (2013) 034910.
113. T. Song, K. C. Han and C. M. Ko, The effect of initial fluctuations on bottomonia suppression in relativistic heavy-ion collisions, arXiv:1112.0613.
114. B.-W. Zhang, C.-M. Ko and W. Liu, *Phys. Rev. C* **77** (2008) 024901.
115. J. Uphoff, K. Zhou, O. Fochler, Z. Xu and C. Greiner, *PoS* **BORMIO2011** (2011) 032.
116. K. Zhou, N. Xu, Z. Xu and P. Zhuang, *Phys. Rev. C* **89**(5) (2014) 054911.
117. N. Topilskaya *et al.*, *Nucl. Phys. A* **715** (2003) 675–678.
118. B. Alessandro *et al.*, *Eur. Phys. J. C* **39** (2005) 335–345.
119. A. Adare *et al.*, *Phys. Rev. Lett.* **98** (2007) 232301.
120. E. Scomparin, Presentation at QM2012 (2012).
121. Y.-P. Liu, Z. Qu, N. Xu, and P.-F. Zhuang, *Phys. Lett. B* **678** (2009) 72–76.
122. K. Olive *et al.*, *Chin. Phys. C* **38** (2014) 090001.
123. M. Schroedter, R. L. Thews and J. Rafelski, *Phys. Rev. C* **62** (2000) 024905.
124. D. Griffiths, *Introduction to Elementary Particles* (Wiley-VCH, Weinheim Germany, 2008).
125. A. Adare *et al.*, *Phys. Rev. D* **82** (2010) 012001.
126. E. T. Atomssa, *Eur. Phys. J. C* **61** (2009) 683–686.
127. J. Lansberg, *Phys. Lett. B* **695** (2011) 149–156.
128. Y. Liu, C. Greiner and C. M. Ko, Spin asymmetry of J/psi in peripheral Pb + Pb collisions at LHC, arXiv:1403.4317.
129. K. Adcox *et al.*, *Nucl. Phys. A* **757** (2005) 184–283.
130. L. Adamczyk *et al.*, *Phys. Lett. B* **722** (2013) 55–62.
131. J.-Y. Ollitrault, *Phys. Rev. D* **46** (1992) 229–245.
132. A. Adare *et al.*, *Phys. Rev. Lett.* **98** (2007) 162301.
133. S. S. Adler *et al.*, *Phys. Rev. Lett.* **91** (2003) 182301.
134. J. Adams *et al.*, *Phys. Rev. Lett.* **95** (2005) 122301.
135. M. Marchisone, *PoS* **EPS-HEP2013** (2013) 185.
136. B. Alessandro *et al.*, *Eur. Phys. J. C* **48** (2006) 329.
137. R. Arnaldi *et al.*, *Phys. Lett. B* **706** (2012) 263–267.
138. Y. Liu, C. M. Ko and T. Song, *Phys. Lett. B* **728** (2014) 437–442.
139. M. Abreu *et al.*, *Nucl. Phys. A* **698** (2002) 127–134.
140. M. Abreu *et al.*, *Phys. Lett. B* **423** (1998) 207–212.
141. B. Alessandro *et al.*, *Eur. Phys. J. C* **49** (2007) 559–567.
142. M. Abreu *et al.*, *Phys. Lett. B* **444** (1998) 516–522.
143. A. Adare *et al.*, *Phys. Rev. Lett.* **98** (2007) 232002.
144. I. Abt *et al.*, *Phys. Lett. B* **561** (2003) 61–72.
145. X. Zhao and R. Rapp, *Phys. Rev. C* **82** (2010) 064905.
146. L. Adamczyk *et al.*, *Phys. Rev. C* **90**(2) (2014) 024906.
147. B. Trzeciak, J/ψ measurements in the STAR experiment, arXiv:1412.7345.
148. A. Adare *et al. Phys. Rev. Lett.* **101** (2008) 122301.

149. T. Song, Y. Park, S. H. Lee and C.-Y. Wong, *Phys. Lett. B* **659** (2008) 621–627.
150. X. Zhao and R. Rapp, Charmonium production at high $p(t)$ at RHIC, arXiv:0806.1239.
151. Y. Liu, N. Xu and P. Zhuang, *Nucl. Phys. A* **834** (2010) 317C–319C.
152. U. W. Heinz and C. Shen, Private communication (2011).
153. H. Liu, *Nucl. Phys. A* **830** (2009) 235c–238c.
154. B. B. Abelev *et al.*, *Phys. Lett. B* **734** (2014) 314–327.
155. S. Chatrchyan *et al.*, *JHEP* **1205** (2012) 063.
156. E. Abbas *et al.*, *Phys. Rev. Lett.* **111** (2013) 162301.
157. E. Scomparin, *Nucl. Phys. A* **904–905** (2013) 202c–209c.
158. D. H. Moon, *Nucl. Phys. A* **910–911** (2013) 215–218.
159. B. Chen, Y. Liu, K. Zhou and P. Zhuang, *Phys. Lett. B* **726** (2013) 725–728.
160. X. Zhao, A. Emerick and R. Rapp, *Nucl. Phys. A* **904–905** (2013) 611c–614c.